

## Atypical periosteal reaction and unusual bone involvement of ameloblastoma: A case report with 8-year follow-up

Pornkawee Charoenlarp<sup>1,\*</sup>, Onanong Silkosessak-Chaiudom<sup>1</sup>, Vichittra Vipismakul<sup>2</sup>

<sup>1</sup>Department of Radiology, Faculty of Dentistry, Chulalongkorn University, Bangkok, Thailand

<sup>2</sup>Department of Oral Pathology, Faculty of Dentistry, Chulalongkorn University, Bangkok, Thailand

### ABSTRACT

Unusual radiographic findings of intraosseous ameloblastoma have been reported and discussed. In the case discussed herein, cone-beam computed tomography (CBCT) clearly showed many radiographic features that were ambiguous on conventional radiographs, including an ill-defined periphery, extensive superficial buccal extension with minimal lingual extension, obvious bucco-crestal expansion, and multiple triangular (Codman's triangle-like) areas of periosteal reaction. Based on the above-mentioned findings, the differential diagnosis was a long-term infected benign or low-grade malignant lesion. An incisional biopsy was performed, and the histopathologic diagnosis was acanthomatous ameloblastoma. Recurrence of the lesion was clearly detected on CBCT images at 4 and 8 years after surgery. These unusual radiographic findings have never been reported to be associated with ameloblastoma, and thus may contribute to novel concepts in radiographic interpretation in the future. This report also underscores the important role played by CBCT as a comprehensive diagnostic tool and for definite confirmation of recurrence. (*Imaging Sci Dent* 2021; 51: 195-201)

**KEY WORDS:** Ameloblastoma; Cone-Beam Computed Tomography; Neoplasms; Periosteum

Based on the 2017 World Health Organization classification of odontogenic and maxillofacial bone tumors, ameloblastoma is the most common type of benign odontogenic tumor excluding odontomas. It originates from the dental lamina, as indicated by the expression of early dental epithelial markers such as paired-like homeodomain transcription factor 2 (PITX2), homeobox protein MSX-2, homeobox protein DLX-2, runt-related transcription factor 1 (RUNX1), and the insulin gene enhancer protein ISL-1.<sup>1</sup> Ameloblastoma occurs most often in the second to fourth decades of life, and in the Thai population it shows a slight male predilection.<sup>2</sup> Clinically, conventional ameloblastoma appears as a locally aggressive, slow-growing, and often asymptomatic lesion. As the tumor enlarges, it may affect adjacent structures, causing tooth displacement, severe bony expansion, and perforation of the cortical plate with subsequent invasion into adjacent soft tissues. Occasionally,

ameloblastoma can cause symptoms such as pain, paresthesia, and/or anesthesia of the affected area other than facial swelling and malocclusion.<sup>3</sup> Its typical radiographic features include unilocular or, more often, multilocular radiolucencies in "soap bubble" or "honeycomb" patterns with well-defined and corticated borders, especially in the mandibular molar or ascending ramus region. Prominent resorption and displacement of adjacent structures are commonly observed.<sup>4</sup> Conventional ameloblastoma presents with a variety of histological subtypes including follicular (the most frequent pattern), plexiform, acanthomatous, basal cell, granular cell and desmoplastic variants. A combination of microscopic patterns can be seen in a large tumor without clinical significance.<sup>5</sup> Various unusual clinical and radiographic findings of intraosseous ameloblastoma, including asymmetric involvement have been reported.<sup>6-8</sup> However, atypical radiographic appearances showing a somewhat ill-defined diffuse margin and periosteal reaction (as seen in infections or malignant lesions) have not been previously reported in the English-language literature. The purpose of this article is to present and discuss a case of

Received September 24, 2020; Revised October 29, 2020; Accepted November 14, 2020  
\*Correspondence to : Dr. Pornkawee Charoenlarp  
Department of Radiology, Faculty of Dentistry, Chulalongkorn University, Henry Dunant Road, Pathumwan District, Bangkok 10330, Thailand  
Tel) 66-2-218-8714, E-mail) Pornkawee.C@chula.ac.th

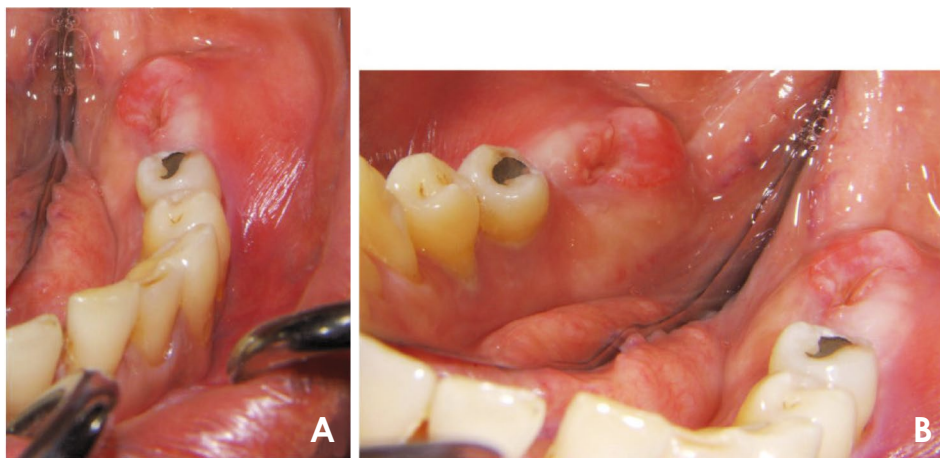


**Fig. 1.** An intraoral examination shows marked buccal expansion and a shallow vestibule extending from the left mandibular second premolar to the retromolar area (A) with mild lingual expansion (B).

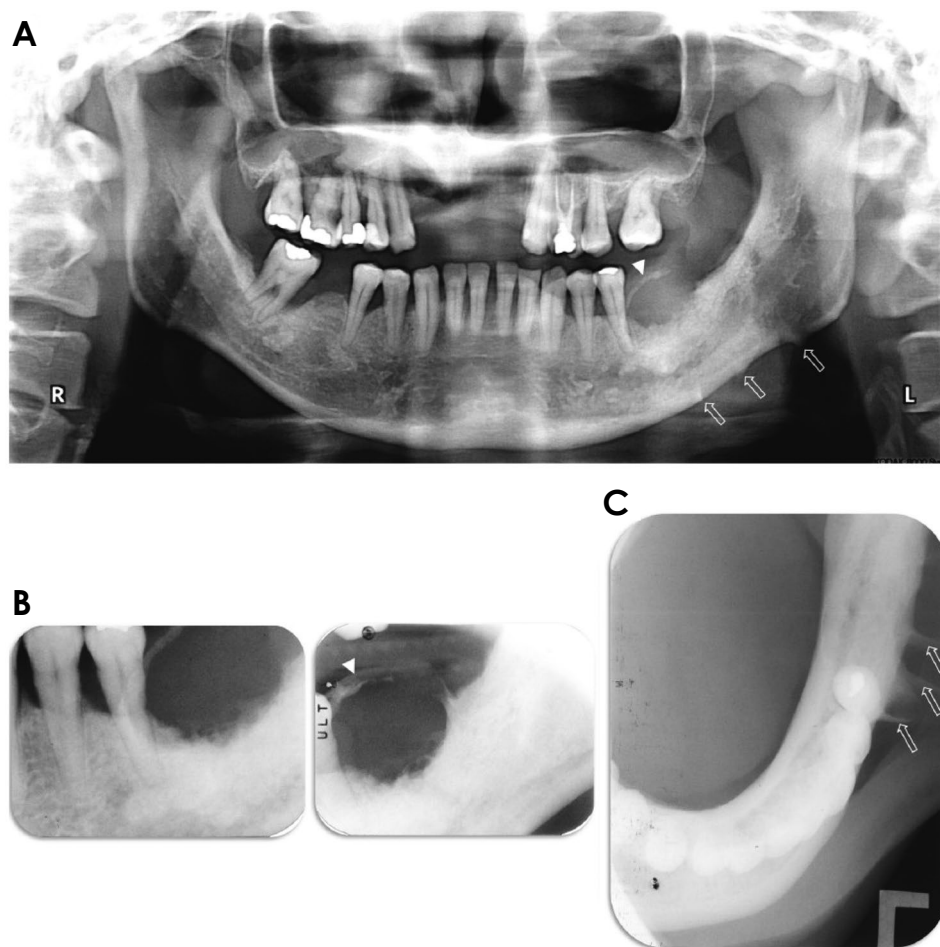


**Fig. 2.** A. A panoramic radiograph reveals ambiguous extension of the lesion. The white arrowhead indicates thick superior cortication with a perforated area in the crestal process and hollow arrows indicate bony projections at the inferior mandibular cortex. B. Periapical radiographs of the left mandibular premolars and molars show widening of the periodontal ligament space around the mandibular second premolar. The white arrowhead shows thick superior cortication in the crestal process. C. Cross-sectional occlusal radiograph of the left mandibular posterior region shows prominent buccal expansion with 3 perpendicular straight bone projections from the buccal surface corresponding to those shown on the panoramic radiograph (hollow arrows).

ameloblastoma with an unusual radiographic appearance, which presented with prominent asymmetric bucco-crestal expansion, an ill-defined margin, and Codman’s triangle-like areas of periosteal reaction. This report also underscores that cone-beam computed tomography (CBCT) is the imaging modality of choice for defining these characteristics.

### Case Report

A 48-year-old Thai man presented to the Faculty of Dentistry, Chulalongkorn University, Bangkok, Thailand with a chief complaint of painless swelling in the mandibular left posterior region in the past 1 year. As prior treatment, he reported surgical removal of an impacted lower left third

molar and simple extraction of a lower left second molar simultaneously due to a large carious cavity 2 years ago. Six months later, gingival swelling adjacent to the extraction site with intermittent clear discharge was noticed. Subsequently, the swelling steadily grew without discharge. He described no history of pain, numbness, or other abnormal sensations. His overall physical status was within normal limits.

Extraoral examination revealed a moderate swelling in the left cheek. No cervical lymphadenopathy was noted. An intraoral examination revealed marked buccal expansion extending from the left mandibular second premolar to the retromolar area with a variable consistency ranging from hard to soft with perforation in some areas (Fig. 1). Neither discharge nor tenderness was detected upon palpation. The overlying mucosa was normal except at the alveolar ridge of the left mandibular second molar, which had indentations from the opposing teeth. The left mandibular second

premolar had first to second degree mobility. The clinical impressions included a cystic lesion or benign tumor with secondary infection. Conventional radiographic examinations (panoramic, cross-sectional occlusal, and periapical radiographs) showed a round radiolucent lesion with prominent crestal expansion in the left mandibular first and second molars (Figs. 2A and 2B) surrounded by wide sclerotic marrow bone in the basal half of the mandible and a slightly compressed inferior alveolar canal. Prominent buccal bone expansion was observed, while additional buccal septation-like projections (Fig. 2C) were detected and correlated with small inferior projections (Fig. 2A) on the inferior border of the mandible on panoramic radiography. Mild overall widening of the periodontal ligament space around the root of the left mandibular second premolar was noted. The initial radiographic impressions included a long-term infected benign or low-grade malignant lesion. It was subsequently decided to perform CBCT, which revealed distinct and



**Fig. 3.** Multiplanar cone-beam computed tomography images, in coronal (A) and axial (B) views, confirm the predominance of bucco-crestal expansion (white arrowhead), while minimal buccal bone involvement and prominent buccal extension to inferior border of mandible are revealed (hollow arrows point at the Codman's triangle-like periosteal reaction).

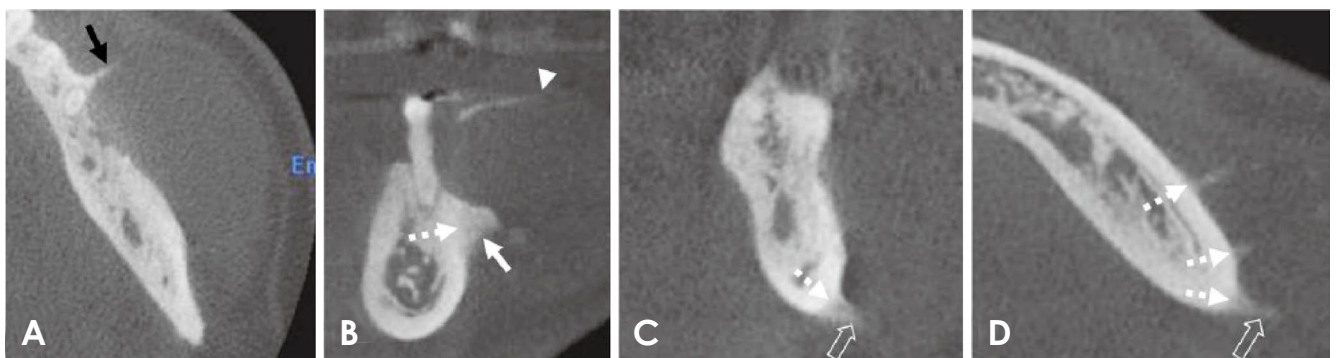


**Fig. 4.** Details illustrating various bone projections in representative CBCT images. A. The black arrow indicates the margin of severe bone expansion manifesting as one of the aforementioned right-angle triangular bone projections in a cross-sectional occlusal view. B. The arrowhead indicates very thin or missing cortication caused by severe expansion of the lesion. B-D. Dotted arrows designate the mandibular original cortex. C and D. Hollow arrows point at the Codman's triangular-like periosteal reaction.

more elaborate information (Figs. 3 and 4), as follows: 1) similar main crestal-buccal involvement (Fig. 3A and 4B; white arrowheads) and severe buccal expansion showing as right-angle thin triangular bone projection at the margin of the lesion (Fig. 4A, black arrow), but with peripheral extension creeping along the buccal cortex down to the inferior border of the mandible, 2) a somewhat infiltrative margin, and 3) Codman's triangle-like areas of periosteal reaction in the buccal and inferior region (Fig. 3A, 3B, 4C and 4D; hollow arrows).

An incisional biopsy was performed and microscopic examination reported multiple islands of tumor consisting of a peripheral layer of ameloblast-like cells showing reverse polarization. These cells enclosed a central core of loosely arranged cells resembling the stellate reticulum. Squamous metaplasia was noted in the central portion of the tumor islands (Fig. 5). The diagnosis was acanthomatous ameloblastoma. The patient underwent en bloc resection and histopathological examination of the whole specimen confirmed the tumor to be acanthomatous ameloblastoma.

Recurrence of the lesion was detected after 4 years of follow-up on a panoramic radiograph and was confirmed using CBCT images. Compared to the immediate post-sur-

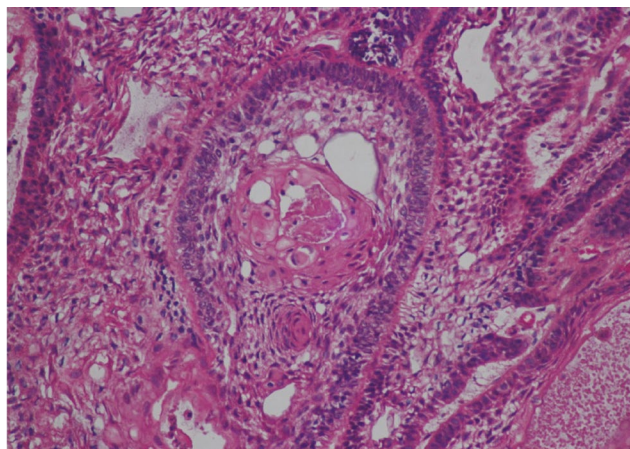


**Fig. 5.** Histopathologic examination of the lesion shows ameloblastic islands with squamous metaplasia in the central cores (H&E stain,  $\times 400$ ).



**Fig. 6.** A postoperative panoramic radiograph taken 1 day after surgery reveals a sharp outline in the crestal portion and a relatively sharp outline in the basal part of the mandibular body.

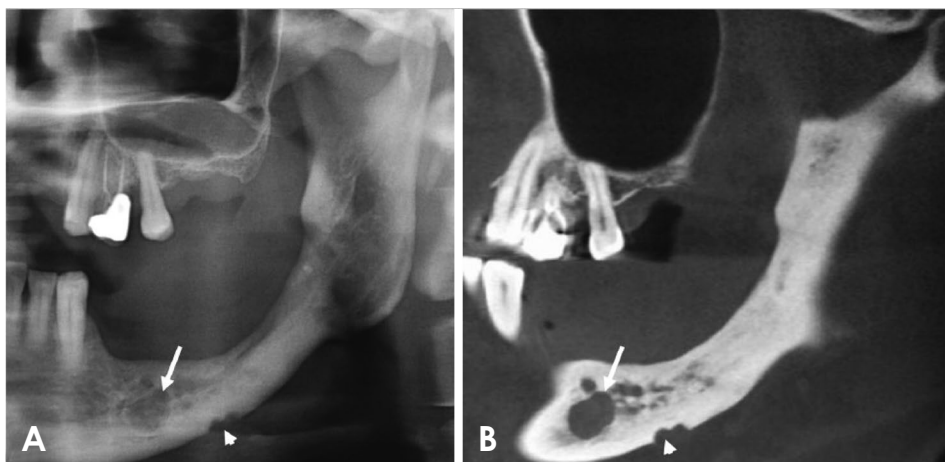


**Fig. 7.** Cropped postoperative panoramic radiograph (A) and corresponding corrected sagittal cone-beam computed tomography image (B) at a 4-year follow up. The arrowheads and arrows show recurrence in the infero-anterior region of the previous site.

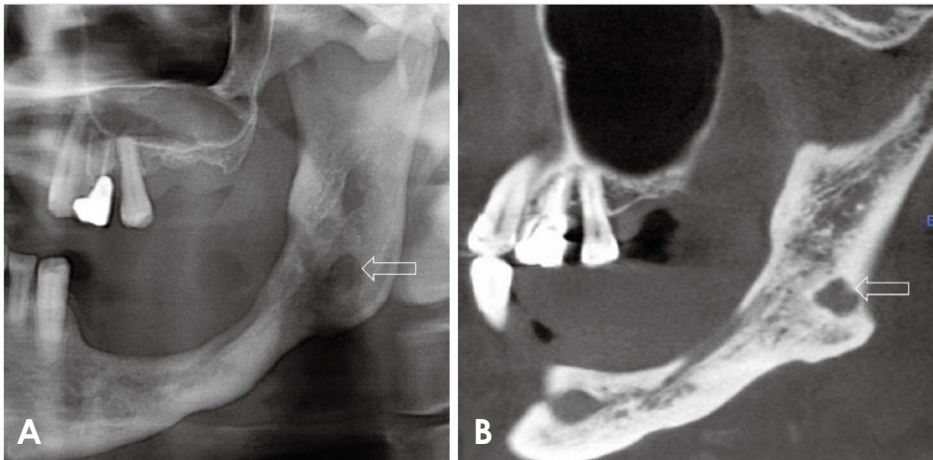


**Fig. 8.** Cropped postoperative panoramic radiograph (A) and corresponding corrected sagittal cone-beam computed tomography image (B) at an 8-year follow up. The hollow arrows show recurrence at the posterior region of the previous site.

gical panoramic radiograph (Fig. 6), the signs of recurrence included a newly developed, saucerized radiolucency with a well-defined margin at the inferior cortex of the left mandible and a somewhat oval-shaped relative radiolucency with a well-defined margin near the mental foramen (Fig. 7). Enucleation was performed due to the patient's needs instead of total resection and the histopathological report was recurrent ameloblastoma.

Four years after enucleation, another oval relative radiolucency with a well-defined margin was detected near the angle of the mandible on panoramic radiography, and was confirmed using CBCT (Fig. 8). The patient again chose to undergo enucleation with peripheral osteotomy.

### Discussion

The differential diagnosis is a systematic process during which one establishes a list of possible diseases or lesions that present similar clinical and/or radiographic features. The important diagnostic information consists of the patient's history, clinical information, radiographic findings, and laboratory results. In this case, due to the unavailability of pre-extraction images, the diagnostic investigation was started based on clinical and radiographic information at the authors' institution. However, it could be speculated that there may have been a pre-existing lesion before tooth extraction. Nevertheless, since the reason for the removal of the mandibular second and third molars was gross caries and impaction without any obvious bone expansion, the Ameloblastoma might not be related to prior tooth extraction or surgical removal. As a result, the first impression of this lesion did not include the possibility that it was a residual lesion.

In bony lesions, the radiographic findings provide impor-

tant and usual signposts for abnormalities. Radiographic impressions can be made with 3 levels of confidence.<sup>9</sup> The highest level of confidence includes specific lesions with a pathognomonic sign, such as compound odontomas. The second group includes lesions with sufficient characteristics for a probable accurate diagnosis such as odontogenic myxoma or dentigerous cyst. In the third level, it is difficult to formulate a differential diagnosis from radiographs alone. The radiographic appearance of ameloblastoma is usually classified in the second group - that is, it should be possible to differentiate ameloblastoma from other conditions. However, the case described herein showed unusual radiographic findings of ameloblastoma, and it fell into the third category, posing a challenge for the radiographic differential diagnosis. Several reports of atypical ameloblastoma have been published, and it is crucial to continue collecting these peculiar manifestations in order to enhance radiographic diagnosis, especially in the era of user-friendly 3-dimensional imaging.

The exceptional superficial buccal involvement of this lesion created an illusion of lesion extension on conventional radiographs. The nature of the lesion was clearly illustrated only on CBCT images, which were suggestive of ectopic progression of this lesion, growing close to crestal and buccal surface of the mandible. Kawai et al.<sup>6</sup> also reported the same characteristics as shown in our case, and had the same diagnostic dilemma from conventional radiographs. These imaging characteristics show a considerable divergence from the common perception that the origin of the tumor is close to the center of the mandible and expands in both buccolingual directions.<sup>5,10,11</sup> This feature might be explained through the general knowledge that ameloblastoma derives from the residues of odontogenic epithelium such as epithelial rests of Malassez, reduced enamel epithelium, or rem-

nants of dental lamina that can remain anywhere else in the tooth-bearing area.<sup>12</sup>

The margin provides information regarding the aggressiveness and growth rate of lesions and the body's response to the lesion. The ill-defined border with an area of a somewhat infiltrative margin surrounded by wide sclerosing bone in this case can be classified as type 1C in Lodwick's classification of lytic bone lesions<sup>13</sup> or grade II in the modified Lodwick-Madewell grading system.<sup>14</sup> For both of these categories, it is recommended to include malignancy in the differential diagnosis and to pursue further imaging (computed tomography or magnetic resonance imaging). The presence of bone sclerosis next to an osteolytic lesion is also considered an important imaging landmark to distinguish infection from malignancy, despite the frequent observation in clinical settings of oral squamous cell carcinoma. The radiographic appearance of this case could represent a spectrum of malignancy, a rapidly growing benign lesion with superimposing infection, or osteomyelitis.<sup>15</sup> However, in light of prominent bone expansion, a rapidly growing benign lesion or benign lesion with infection was considered more likely. The wide zone of sclerotic bone beyond the ill-defined radiolucency was most likely to be a previous reaction of the host bone to low-grade chronic infection,<sup>16</sup> corresponding to the early clinical presentation of on-and-off swelling with clear discharge.

Codman's periosteal reaction refers to a triangular area of new bone formation at the periphery of cortical bone destruction.<sup>17</sup> Generally, periosteal new bone formation arises after the periosteum is stripped from the cortex by various causes such as tumors, infection, trauma, drug-induced responses, and some arthritic conditions.<sup>18</sup> The pattern of periosteal reaction is determined by the intensity, aggressiveness, and duration of the underlying lesion and is useful for formulating a differential diagnosis.<sup>17,19,20</sup> The pattern identified herein is classified as an aggressive form of periosteal reaction,<sup>18</sup> and commonly seen in malignant lesions such as osteosarcoma. However, it occasionally found in metastases and aggressive benign entities that lift the periosteum such as infection and subperiosteal hematoma,<sup>15,18</sup> and only 1 report<sup>21</sup> showed a radiographic finding of benign tumor (central odontogenic fibroma) having a Codman's triangle periosteal reaction. No previous studies have reported ameloblastoma showing Codman's triangle-like periosteal reaction, as presented in this case. The causes for this finding may be the aggressiveness of lesion itself or the concomitant infection.

The application of CBCT is another aspect that deserves emphasis, as CBCT undoubtedly discloses details of the lesion and facilitates an accurate differential diagnosis. At

present, the increasing availability of CBCT in the dental diagnostic field provides radiologists with insights into the morphological characteristics and extent of these lesions. In the future, other novel interesting radiographic findings may be observed, such as the Codman's triangle-like periosteal reaction in intraosseous ameloblastoma described herein. These contributions will create new knowledge and may change previous concepts of radiographic interpretation. CBCT is also helpful for the follow-up of patients with unclear conventional images for the early detection of suspected recurrence, as shown in this case. In conclusion, this report showed unusual radiographic findings of ameloblastoma associated with asymmetric bucco-crestal expansion, ill-defined sclerotic margin, and Codman's triangle-like areas of periosteal reaction. Advanced imaging modalities such as CBCT are highly recommended to provide more accurate details than the indistinct findings seen on conventional radiographs.

**Conflicts of Interest:** None

## References

1. Vered M, Muller S, Heikinheimo K. Benign epithelial odontogenic tumours. In: El-Naggar AK, Chan JK, Rubin Grandis J, Takata T, Slootweg P. WHO classification of head and neck tumours. 4th ed. Lyon: International Agency for Research on Cancer; 2017. p. 215-7.
2. Intapa C. Analysis of prevalence and clinical features of ameloblastoma and its histopathological subtypes in southeast Myanmar and lower northern Thailand populations: a 13-year retrospective study. *J Clin Diagn Res* 2017; 11: ZC102-6.
3. Becelli R, Carboni A, Cerulli G, Perugini M, Iannetti G. Mandibular ameloblastoma: analysis of surgical treatment carried out in 60 patients between 1977 and 1998. *J Craniofac Surg* 2002; 13: 395-400.
4. Baghdady M. Principles of radiographic interpretation. In: White SC, Pharoah MJ. Oral radiology: principles and interpretation. 7th ed. St. Louis: Elsevier; 2014. p. 271-84.
5. Black CC, Addante RR, Mohila CA. Intraosseous ameloblastoma. *Oral Surg Oral Med Oral Pathol Oral Radiol Endod* 2010; 110: 585-92.
6. Kawai T, Kishino M, Hiranuma H, Sasai T, Ishida T. A unique case of desmoplastic ameloblastoma of the mandible: report of a case and brief review of the English language literature. *Oral Surg Oral Med Oral Pathol Oral Radiol Endod* 1999; 87: 258-63.
7. Katsura K, Maruyama S, Suzuki M, Saku T, Takagi R, Hayashi T. A case of desmoplastic ameloblastoma arising in the maxillary alveolus: the origin and time-course changes in the early stage of tumour development observed on dental radiographs. *Dentomaxillofac Radiol* 2011; 40: 126-9.
8. Ide F, Mishima K, Yamada H, Kikuchi K, Saito I, Kusama K. Intraosseous ameloblastoma with a prominent extraosseous com-

- ponent: pitfalls in diagnosis. *Head Neck Pathol* 2010; 4: 192-7.
9. Langlais R, Langland OE, Nortje CJ. *Diagnostic imaging of the jaw*. Baltimore: Williams and Wilkins; 1995.
  10. Gümgüm S, Hoşgören B. Clinical and radiologic behaviour of ameloblastoma in 4 cases. *J Can Dent Assoc* 2005; 71: 481-4.
  11. Kaffe I, Buchner A, Taicher S. Radiologic features of desmoplastic variant of ameloblastoma. *Oral Surg Oral Med Oral Pathol* 1993; 76: 525-9.
  12. Ide F, Obara K, Yamada H, Mishima K, Saito I, Horie N, et al. Hamartomatous proliferations of odontogenic epithelium within the jaws: a potential histogenetic source of intraosseous epithelial odontogenic tumors. *J Oral Pathol Med* 2007; 36: 229-35.
  13. Lodwick GS. Radiographic diagnosis and grading of bone tumors, with comments on computer evaluation. *Proc Natl Cancer Conf* 1964; 5: 369-80.
  14. Caracciolo JT, Temple HT, Letson GD, Kransdorf MJ. A modified Lodwick-Madewell grading system for the evaluation of lytic bone lesions. *AJR Am J Roentgenol* 2016; 207: 150-6.
  15. Miller TT. Bone tumors and tumorlike conditions: analysis with conventional radiography. *Radiology* 2008; 246: 662-74.
  16. Whaites E, Drage N. *Radiography and radiology for dental care professionals*. 3rd ed. Oxford: Churchill Livingstone; 2013.
  17. Ida M, Tetsumura A, Kurabayashi T, Sasaki T. Periosteal new bone formation in the jaws. A computed tomographic study. *Dentomaxillofac Radiol* 1997; 26: 169-76.
  18. Rana RS, Wu JS, Eisenberg RL. Periosteal reaction. *AJR Am J Roentgenol* 2009; 193: W259-72.
  19. Greenfield GB. Cardinal roentgen features. In: Greenfield GB. *Radiology of bone diseases*. 5th ed. Philadelphia: JB Lippincott; 1990. p. 405-578.
  20. Mira JM, Picci P, Gold RH. *Bone tumors: clinical, radiologic, and pathologic correlations*. Philadelphia: Lea and Febiger; 1989.
  21. Anbiaee N, Ebrahimnejad H, Sanaei A. Central odontogenic fibroma (simple type) in a four-year-old boy: atypical cone-beam computed tomographic appearance with periosteal reaction. *Imaging Sci Dent* 2015; 45: 109-15.